FEBS 29388 FEBS Letters 579 (2005) 1961–1967

Evidence for major structural changes in subunit C of the vacuolar ATPase due to nucleotide binding

Andrea Armbrüster[a], Christina Hohn[a], Anne Hermesdorf[b], Karin Schumacher[b], Michael Börsch[c], Gerhard Grüber[a,*]

[a] *Universität des Saarlandes, Fachrichtung 2.5 – Biophysik, Universitätsbau 76, D-66421 Homburg, Germany*
[b] *Universität Tübingen, ZMBP-Pflanzenphysiologie, D-72076 Tübingen, Germany*
[c] *3. Physikalisches Institut, Universität Stuttgart, Pfaffenwaldring 57, D-70569 Stuttgart, Germany*

Received 20 January 2005; revised 14 February 2005; accepted 14 February 2005

Available online 25 February 2005

Edited by Stuart Ferguson

Abstract The ability of subunit C of eukaryotic V-ATPases to bind ADP and ATP is demonstrated by photoaffinity labeling and fluorescence correlation spectroscopy (FCS). Quantitation of the photoaffinity and the FCS data indicate that the ATP-analogues bind more weakly to subunit C than the ADP-analogues. Site-directed mutagenesis and N-terminal sequencing of subunit C from *Arabidopsis* (VHA-C) and yeast (Vma5p) have been used to map the C-terminal region of subunit C as the nucleotide-binding site. Tryptophan fluorescence quenching and decreased susceptibility to tryptic digestion of subunit C after binding of different nucleotides provides evidence for structural changes in this subunit caused by nucleotide-binding.

Keywords: Vacuolar-type ATPase; V_1V_0 ATPase; V_1 ATPase; Vma5p; VHA-C; Photoaffinity labeling; Fluorescence correlation spectroscopy

1. Introduction

The vacuolar ATPase (V_1V_0 ATPase) is an electrogenic ion pump found throughout every eukaryotic cell. This enzyme harnesses the energy derived from ATP hydrolysis to pump ions across membranes, creating an electrochemical gradient. V-ATPases have two structural and functional parts, a peripheral V_1 complex, whose catalytic part faces the cytosol, and a membrane bound, ion conducting V_0 part [1]. The eukaryotic enzyme V_1 consists of eight subunits A–H, whereas the V_0 domain is composed of the four different subunits a, c, d and e [2]. ATP is hydrolyzed on the V_1-headpiece, composed of an A_3:B_3 hexamer, and the energy released during that process is transmitted to the membrane-bound V_0 domain, to drive ion translocation. This energy coupling occurs via the so-called ''stalk'' structure, an assembly of the V_1 and V_0 subunits C–H and *a*, respectively, that forms the functional and structural interface [3].

A characteristic feature of the eukaryotic V_1V_0 ATPase is the regulation by reversible disassembly of the V_1 and V_0 subcomplexes [4,5], resulting in the decrease of Mg^{2+}-dependent ATPase activity and proton pumping across the membrane. Reassembly of both domains restores these activities. It was shown that subunits C and H are important for inhibition of the Mg^{2+}-dependent ATPase activity of dissociated V_1 complexes [6]. The high-resolution structure of the H subunit [7] and data on the gross structure of the V_1V_0 ATPase complexes suggest that in the intact enzyme this subunit is involved in the formation of the peripheral stalk region [8], despite the fact that a rearrangement within the disassembled V_1 is possible [9,10]. Electron microscopy studies of the disassembled V_1 complex from tobacco hornworm *Manduca sexta* have shown that subunit C dissociates from the V_1 subcomplex [11], although it is essential for the reassembly of the functional V_1V_0 [9,12]. Previously, the structure of the C subunit (Vma5p) from the yeast V_1V_0 ATPase has been studied by small angle X-ray scattering, revealing that the hydrated Vma5p has an elongated boot-shaped structure with a maximum size of 12.5 nm [13]. A recent 1.75 Å map from X-ray diffraction studies of Vma5p [14] confirms this feature and shows that this subunit consists of three distinct domains. An upper head domain, composed of the amino acids 166–263, a large globular foot, consisting of the N- and C-termini, and an elongated neck domain, which connects the head and foot region (Fig. 1).

An intriguing result was the formation of a stable and ATPase active hybrid complex composed of Vma5p and V_1 from *M. sexta*, lacking endogenous subunit C. It has been demonstrated that the addition of recombinant subunit C to the V_1(-C) complex significantly increased ATPase activity [13], supporting its functional role in regulation of ATPase activity [15,16]. Here, we report for the first time the property of nucleotide binding of subunit C, independently observed by photoaffinity labeling and fluorescence correlation spectroscopy (FCS). Decreased tryptophan fluorescence and trypsin susceptibility in the presence of different nucleotides are discussed in the light of structural alterations in subunit C and its important role in the control of the V_1V_0 holoenzyme.

*Corresponding author. Fax: +49 0 6841 162 6086.
E-mail address: ggrueber@med-rz.uni-saarland.de (G. Grüber).

Abbreviations: BODIPY-FL-ATP, BODIPY® FL 2′-(or-3′)-*O*-(*N*-(2-aminoethyl)urethane); IPTG, isopropyl-β-D-thio-galactoside; 8-N_3-3′-biotinyl-ATP, 8-azido-3′(2′)-biotinyl adenosine 5′-diphosphate; 8-N_3-3′-biotinyl-ATP, 8-azido-3′(2′)-biotinyl adenosine 5′-triphosphate; NTA, nitrilotriacetic acid; PAGE, polyacrylamide gel electrophoresis; PCR, polymerase chain reaction; SDS, sodium dodecyl sulfate; Tris, Tris-(hydroxymethyl)aminomethane

0014-5793/$30.00
doi:10.1016/j.febslet.2005.02.042

Fig. 1. Structure of subunit C (Vma5p). The atomic model derived from the X-ray coordinates kindly provided by Prof. N. Nelson, Tel Aviv University [14]. The head-region I_{178}–S_{263} (blue) and both the N-(L5–G_{56}) and C-terminus (G_{320}–M_{357}, Y_{382}–L_{392}) are labeled in yellow. The disordered region in-between the amino acids 357–382 are indicated by the residues M357 (magenta) and Y382 (red).

2. Materials and methods

2.1. Biochemicals

ProofStart™ DNA Polymerase and Ni^{2+}–NTA-chromatography resin were received from Qiagen (Hilden or Novagen, Bad Soden, Germany); restriction enzymes were purchased from MBI Fermentas (St. Leon-Rot, Germany). Chemicals for gel electrophoresis were received from Serva (Heidelberg, Germany). All other chemicals were at least of analytical grade and received from BIOMOL (Hamburg, Germany), Merck (Darmstadt, Germany), Roth (Karlsruhe, Germany), or Sigma (Deisenhofen, Germany).

2.2. Expression and purification of subunit C from Arabidopsis thaliana (VHA-C) and Saccharomyces cerevisiae (Vma5p)

To amplify the coding region of *VHA-C*, oligonucleotide primers 5′-ataggatccatgacttcgagatattgggt-3′ (forward primer) and 5′-atactcgagttaagcaaggttgatagt-3′ (reverse primer), incorporating *Bam*HI and *Xho*I restriction sites, respectively (underlined), were designed. *A. thaliana* (ecotype Col- 0) cDNA was used as template for the polymerase chain reaction (PCR). Following digestion with *Bam*HI and *Xho*I, the PCR product was ligated into the pET28a vector (Novagen, Bad Soden, Germany). The pET28a vector containing the *VHA-C* insert was then transformed into *Escherichia coli* cells (strain BL21DE3) (Novagen, Bad Soden, Germany) and grown on 50 μg/ml kanamycin-containing Luria–Bertoni (LB) agar-plates. To express His_6-VHA-C, liquid cultures were shaken in LB medium-containing kanamycin (50 $\mu g\,ml^{-1}$) for about 2 h at 37 °C until an optical density OD_{600} of 0.6–0.7 was reached. To induce expression of His_6-VHA-C, the cultures were supplemented with isopropyl-β-D-thio-galactoside to a final concentration of 0.2 mM. Following incubation for another 7 h at 20 °C, the cells were harvested at $4500 \times g$ for 20 min, 4 °C. Subsequently, they were lysed by sonication for 6×10 s in buffer A [50 mM Tris-(hydroxymethyl)aminomethane (Tris)/HCl, pH 8, 300 mM NaCl, 10 mM imidazol, 1× Complete inhibitor mix (Roche, Mannheim, Germany)]. The lysate was cleared by centrifugation at $10\,000 \times g$ for 30 min at 4 °C, the supernatant was passed through a filter (0.45 μm pore-size) and supplemented with Ni^{2+}–NTA resin. The His-tagged protein was allowed to bind to the matrix for 60 min at room temperature and eluted with 125 mM imidazole in buffer A. Fractions containing His_6-VHA-C were identified by sodium dodecyl sulfate–polyacrylamide gel electrophoresis (SDS–PAGE), pooled and concentrated using spin concentrators (10 kDa molecular mass cut off; Vivascience, Göttingen, Germany). Wild type VHA-C protein was applied to a Superdex 200 column (Amersham Biosciences), equilibrated in a buffer of 25 mM Tris/HCl (pH 7.5) and then concentrated. The purity of the protein sample was analyzed by SDS–PAGE. Subunit C (Vma5p) of the *S. cerevisiae* V-ATPase was produced and purified according to Armbrüster et al. [13]. Protein concentrations were determined by the bicinchoninic acid assay (BCA; Pierce, Rockford, IL, USA).

2.3. Site-directed mutagenesis

Mutant constructs were produced by PCR-based site-directed mutagenesis using VHA-C in pET28a as template. The following oligonucleotides were used: S211Gfwd 5′-gattatgtggttcctaggggctcgaagaaattg-3′ and S211Grev 5′-caattttcttcgagcccctaggaaccacataatc-3′, S212Gfwd 5′-tatgtggttcctaggtccgggaagaaattgtttg-3′ and S212Grev 5′-caaacaatttcttcccggaaccacata-3′, P312Afwd 5′-gagatacggtttagctccggcgttcttggcatg-3′ and P312Arev 5′- catgccaagaacgccggagctaaaccgtatctc-3′, and R308AY309Afwd 5′-cgctgagagcattatggcagccggtttacctcggcgttc-3′ and 5′-gaacgccggaggtaaaccggctgccataatgctctcagcg-3′. Presence of the mutations was confirmed by sequencing. The VHA-C mutant proteins were prepared as the VHA-C wild type protein described above.

2.4. Photoaffinity labeling

Photoaffinity labeling was performed as described by Schäfer et al. [17]. Protein (8 mg/ml) was incubated with 5×10^{-5} M 8-N_3-3′-biotinyl-ATP (8-azido-3′(2′)-biotinyl adenosine 5′-triphosphate) or 8-N_3-3′-biotinyl-ADP in Tris/HCl buffer (50 mM, pH 8.5, and 100 mM NaCl) for 5 min at 4 °C in the dark followed by irradiation with an ultraviolet lamp at 366 nm for 30 min on ice. The protein sample was analyzed by SDS–PAGE and the gel was stained with Coomassie Brilliant Blue G250. The identification of the labeled subunits was done by Western immunoblots according to Towbin et al. [18] using a streptavidin/POD conjugate for the visualization of the biotinylated proteins. The 8-N_3-3′-biotinyl-ATP and 8-N_3-3′-biotinyl-ADP was a generous gift of Prof. H.-J. Schäfer (Johannes-Gutenberg Universität, Mainz, Germany).

2.5. Chemical cleavage of photoaffinity-labeled Vma5p

The photolabeled Vma5p was incubated overnight in darkness with 10 mg/ml CNBr in 80% formic acid at room temperature. After the incubation period, the sample was dried using a vacuum concentrator (SC 110, Savant), redissolved in buffer (100 mM Tris/HCl) and analyzed directly by electrophoresis. The identification of the labeled fragments was done by Western immunoblots and the use of a streptavidin/POD conjugate as described above. For the N-terminal sequencing, CNBr-generated peptide fragments were blotted on a polyvinylidene difluoride membrane (pore size 0.45 μm) according to [19]. The protein bands, correlating to the labeled fragments, were excised from the membrane and sequenced with a model 473A sequencer from Applied Biosystems.

2.6. Fluorescence correlation spectroscopy

For investigation of ATP- and ADP-binding to subunit C the ATP-analogues BODIPY-FL-ATP (BODIPY® FL 2′-(or-3′)-*O*-(*N*-(2-aminoethyl)urethane) adenosine 5′-triphosphate, Molecular Probes), and

Atto-532-ADP, (Atto-tec, Siegen, Germany) were used. FCS data were recorded in 50 mM Tris/HCl, pH 8.5 and 100 mM NaCl with the fluorophore concentration of approximately 100 pM, 3.8 mM $CaCl_2$, and protein concentrations between 7 and 410 μM, respectively. The fluorescence of single molecules was measured with a confocal setup of local design based on an inverted microscope (IX71; Olympus) similar to [20,21]. Fluorescence excitation with epi-illumination was performed with an argon ion laser (Spectra Physics, Germany) at 488 nm for BODIPY-FL-ATP, or 514,5 nm for Atto-532-ADP, respectively. The laser intensity was attenuated to 150 μW and focused by a water immersion objective (UPlanApo, 60×, NA 1.2; Olympus, Tokyo, Japan) to a measurement volume of 5.3 fl. The fluorescence signal was detected by a single photon counting avalanche photodiode (SPCM-AQR-14; EG & G, Vaudreuil, Canada) after passing an interference filter HQ532/70 for BODIPY-FL-ATP, or HQ585/80 for Atto-532-ADP (AHF, Tübingen, Germany). FCS data were recorded by a real-time correlator PC card (ALV-5000/E; ALV, Langen, Germany) with a measurement time of 300 s. The samples were measured on a microscope slide with a small depression covered with a conventional cover glass. All measurements were performed at 20 °C. These data were quantitatively interpreted using the autocorrelation function [22]:

$$g^{(2)}(t_c) = \frac{1}{N_F} \times \left\{ \alpha \left(\frac{1}{1 + t_c/t_{D_1}} \right) \left(\frac{1}{1 + (\omega_0/z_0)^2 (t_c/t_{D_1})} \right)^{\frac{1}{2}} + (1-\alpha) \left(\frac{1}{1 + t_c/t_{D_2}} \right) \left(\frac{1}{1 + (\omega_0/z_0)^2 (t_c/t_{D_2})} \right)^{\frac{1}{2}} \right\} \times \{1 - T + T \exp(-t_c/t_T)\} \quad (3)$$

Here, N_F is the average number of fluorescent molecules in the confocal volume, $t_{D_1} = \omega_0^2/4D_1$ is the characteristic time for translational diffusion of the molecules with the diffusion coefficient D_1, $t_{D_2} = \omega_0^2/4D_2$ is the characteristic diffusion time for the molecules with diffusion coefficient D_2, T is the average fraction of molecules in the excited triplet state with a characteristic triplet correlation time, t_T, α is the fraction of molecules with the shorter diffusion time t_{D_1}, and ω_0 and z_0 are the radial and axial $1/e^2$ radii of the laser focus and detection volume.

2.7. Tryptophan fluorescence measurements

The intrinsic tryptophan fluorescence was recorded at room temperature using a Varian Cary Eclipse spectrofluorimeter. The protein samples were excited at 295 nm, and the emission was recorded from 300 to 370 nm. Excitation and emission bandpass were set to 5 nm.

2.8. Trypsin digestion studies

Subunit C (8 mg/ml) was incubated with trypsin in a ratio of 320:1 (w/w) in 50 mM Tris/HCl (pH 8.5) and 100 mM NaCl in the absence or presence of 2 mM nucleotide at 30 °C. Trypsin cleavage was stopped by addition of the protease inhibitor Pefabloc SC (8 mM). Peptides were separated by SDS–PAGE [31]. Relative intensities of the protein bands of subunit C at each time-point and under the nucleotide-conditions described were determined by scanning the gel of panel A with an HP (*ScanJet 4c*) flat-bed scanner. The intensity of each protein band was digitized and calculated by the program AIDA 2.40 (advanced image analyzer; RAYTEST).

3. Results

3.1. Nucleotide binding of subunit C

Subunit C is believed to be an ideal candidate for regulating the disassembly of the V-ATPase in response to glucose deprivation [5,12]. As yet the nature of this signal is not clear. Therefore, we hypothesized that subunit C might act as a sensor for cellular ADP:ATP level and tested the capability of C

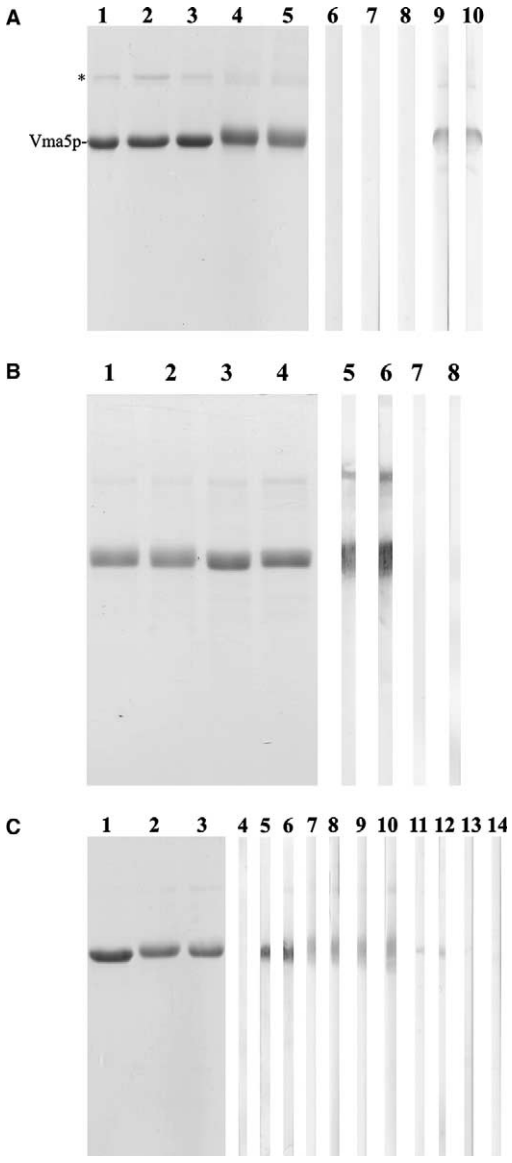

Fig. 2. Photoaffinity labeling subunit C (Vma5p) by 8-N_3-3′-biotinyl-ADP and 8-N_3-3′-biotinyl-ATP. (A) An SDS–PAGE [31] of subunit C (lane 1), irradiated in the absence (lane 3) or presence of 5×10^{-5} M 8-N_3-3′-biotinyl-ATP (lane 4) or Ca-8-N_3-3′-biotinyl-ATP (lane 5). Lane 2, dark control in the presence of 5×10^{-5} M of Ca-8-N_3-3′-biotinyl-ATP. (∗) indicates a slight amount of Vma5p-dimerization, formed by the single residue Cys_{340} of Vma5p in the absence of DTT. (Lanes 6–10) Western blot of the same samples with a streptavidin/POD conjugate to detect the subunit labeled with 8-N_3-3′-biotinyl-ATP. (B), SDS–PAGE [31] and Western blot signal after photoaffinity labeling of Vma5p by 5×10^{-5} M 8-N_3-3′-biotinyl-ADP in the absence (lanes 1 and 5) and presence (lanes 3 and 7) of 1 mM CaADP. Labeling of Vma5p by Ca-8-N_3-3′-biotinyl-ADP in the absence (lanes 2 and 6) and presence (lanes 4 and 8) of 1 mM CaADP. (C) Photoaffinity labeling of wild type VHA-C and the VHA-C mutants S221G, S223G, R318A:Y319A and P322A (numbering of analogous*S. cerevisiae*). Lanes 1 and 4, Dark control in the presence of Ca-8-N_3-3′-biotinyl-ADP; lanes 2 and 5, VHA-C labeled by 5×10^{-5} M Ca-8-N_3-3′-biotinyl-ADP; *lane, 3, 6*, VHA-C labeled by 5×10^{-5} M Ca-8-N_3-3′-biotinyl-ATP. Western blot signals of the VHA-C mutant S221G (lanes 7 and 8), S223G (lanes 9 and 10), R318A:Y319A (lanes 11 and 12) and P322A (lanes 13 and 14) labeled by Ca-8-N_3-3′-biotinyl-ATP and Ca-8-N_3-3′-biotinyl-ADP, respectively.

to bind ADP and ATP. For this purpose, the photoaffinity nucleotide analogues 8-N_3-3′-biotinyl-ADP and 8-N_3-3′-biotinyl-ATP were used, whose specificity for nucleotide binding sites is well documented [23]. As can be seen in Fig. 2A irradiation of subunit C (Vma5p) in the presence of either 8-N_3-3′-biotinyl-ATP or Ca-8-N_3-3′-biotinyl-ATP resulted in a diffuse band, which migrated slightly slower in SDS–PAGE, compared to the defined band of the untreated protein (lane 1). Irradiation of Vma5p in the absence of the label (light control) or incubation of the protein with Ca-8-N_3-3′-biotinyl-ATP in the dark (dark control) resulted in a defined band (Fig. 2A, lanes 2 and 3). The bound photoaffinity label, 8-N_3-3′-biotinyl-ATP, was identified using a streptavidin/POD conjugate, which visualized the biotinylated protein. The immunoblot in Fig. 2A yields the labeling of Vma5p in the presence of either 8-N_3-3′-biotinyl-ATP (lane 9) or Ca-8-N_3-3′-biotinyl-ATP (lane 10), whereby no labeling occurs in the dark (lane 7) and light control (lane 8). These results point to a specific covalent binding of 8-N_3-3′-biotinyl-ATP, indicated by the migration of the same samples in the SDS–PAGE described above. Irradiation of Vma5p in the presence of either 8-N_3-3′-biotinyl-ADP (Fig. 2B, lanes 1 and 5) or Ca-8-N_3-3′-biotinyl-ADP (lanes 2 and 6), resulted in covalent binding of the nucleotide analogue. To test whether the labeling could be protected by a competing nucleotide, ADP and CaADP was added prior to the labeling procedure, respectively. The presence of ADP (Fig. 2B, lanes 3 and 7) and CaADP (lanes 4 and 8) prevented binding of 8-N_3-3′-biotinyl-ADP or Ca-8-N_3-3′-biotinyl-ADP.

In order to prove, whether the nucleotide-binding nature of subunit C is common to other sources, the interaction of the monofunctional labels 8-N_3-3′-biotinyl-ATP and 8-N_3-3′-biotinyl-ADP with subunit C (VHA-C) of *A. thaliana* was analyzed. As demonstrated in Fig. 2C, SDS–PAGE and streptavidin/POD conjugate detection of the irradiated VHA-C revealed that 8-N_3-3′-biotinyl-ATP (lanes 2 and 5) or 8-N_3-3′-biotinyl-ADP (lanes 3 and 6) bound to subunit C, respectively. The specificity of nucleotide-binding was studied using the VHA-C mutants R318, Y319 and P322 (numbering of analogous *S. cerevisiae* residues), which are highly conserved among most eukaryotes, and the mutants S221G and S223G, localized in the head domain of subunit C (Fig. 1). As detected by the streptavidin/POD conjugate the VHA-C mutants S221G and S223G were covalently labeled by Ca-8-N_3-3′-biotinyl-ATP and Ca-8-N_3-3′-biotinyl-ADP comparable to wild type VHA-C (Fig. 2C, lanes 7–10). By comparison, a significantly decreased amount of bound nucleotide-analogues can be detected using the VHA-C double mutant R318A:Y319A (lanes 11–12), whereas neither Ca-8-N_3-3′-biotinyl-ATP nor Ca-8-N_3-3′-biotinyl-ADP showed labeling of the VHA-C single mutant P322A (lanes 13–14).

3.2. Location of the nucleotide-binding site in subunit C

Subunit C (Vma5p) photolabeled with 8-N_3-3′-biotinyl-ADP was digested with CNBr, which cleaves at the COOH terminus of methionine residues, followed by resolution on an SDS–PAGE (Fig. 3) and Western blotting. Two specifically labeled bands with apparent molecular masses of 28.6 and 4.1 kDa were visible in the blot (Fig. 3, lane 2). N-terminal sequence analysis, resulting in the sequences $_{106}$P V P E Y L E N F Q and $_{358}$K D K K G K I N, indicated that the labeled CNBr-fragments consisted of the C-terminal peptides P_{106}–L_{392} and K_{358}–L_{392}. The same marked peptides were detected after CNBr-treatment of the 8-N_3-3′-biotinyl-ATP labeled Vma5p (data not shown), demonstrating that the nucleotide-binding site is located at the C-terminus of Vma5p.

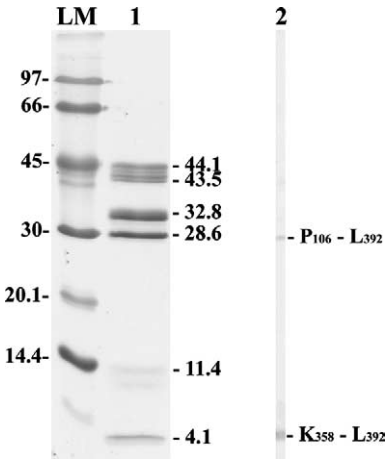

Fig. 3. CNBr cleavage of Ca-8-N_3-3′-biotinyl-ADP Vma5p. Vma5 was photoaffinity-labeled with Ca-8-N_3-3′-biotinyl-ADP and subjected to treatment with CNBr. The labeled and cleaved protein was analyzed by SDS–PAGE (*lane 1*) followed by Western blotting. The labeled peptides were marked by the streptavidin/POD conjugate (lane 2).

3.3. Nucleotide-binding of subunit C characterized by FCS

ATP/ADP-binding of subunit C and the strength of the nucleotide-binding were further examined by FCS, which is a highly sensitive tool to determine binding/dissociation equilibria in the nanomolar range. The characteristic diffusion time, t_D, for subunit C (Vma5p) was measured by selectively labeling of the protein with tetramethylrhodamine-5-maleimide (TMR) at the Cys_{340}. The diffusion times of the labeled Vma5p were compared to the standard fluorophore rhodamine R6G and the fluorescent ADP-derivative Atto-532-ADP (Fig. 4A). The mean count rate per TMR fluorophore bound to subunit C was 20 kHz compared to 39.5 kHz for Atto-532-ADP, and 56 kHz for R6G in these FCS-experiments. Fitting the autocorrelation functions resulted in characteristic times of diffusion $t_D = 1.2$ ms for Vma5p-TMR, $t_D = 0.28$ ms for Atto-532-ADP, and $t_D = 200$ μs for R6G.

Fig. 4B shows the measured autocorrelation curves of the fluorescent ADP-analogue, Atto-532-ADP in the absence and presence of Vma5p. The addition of subunit C resulted in a significant change of the mean diffusion time t_D, which increased up to 36% with increasing concentrations of subunit C. This confirmed that Atto-532-ADP bound to Vma5p in the presence of Ca^{2+}. Using the relation $t_D = \omega_0^2/4D$, between the radial $1/e^2$ radius, $\omega_0 = 470$ nm, and the characteristic translational diffusion time, t_D, the translational diffusion coefficient, D, of Atto532-ADP in the absence of Vma5p was determined to be $(2 \pm 0.1) \times 10^{-6}$ cm^2/s, and for Vma5p-TMR $(4.7 \pm 0.4) \times 10^{-7}$ cm^2/s, respectively, related to a diffusion coefficient of 2.8×10^{-6} cm^2/s of R6G

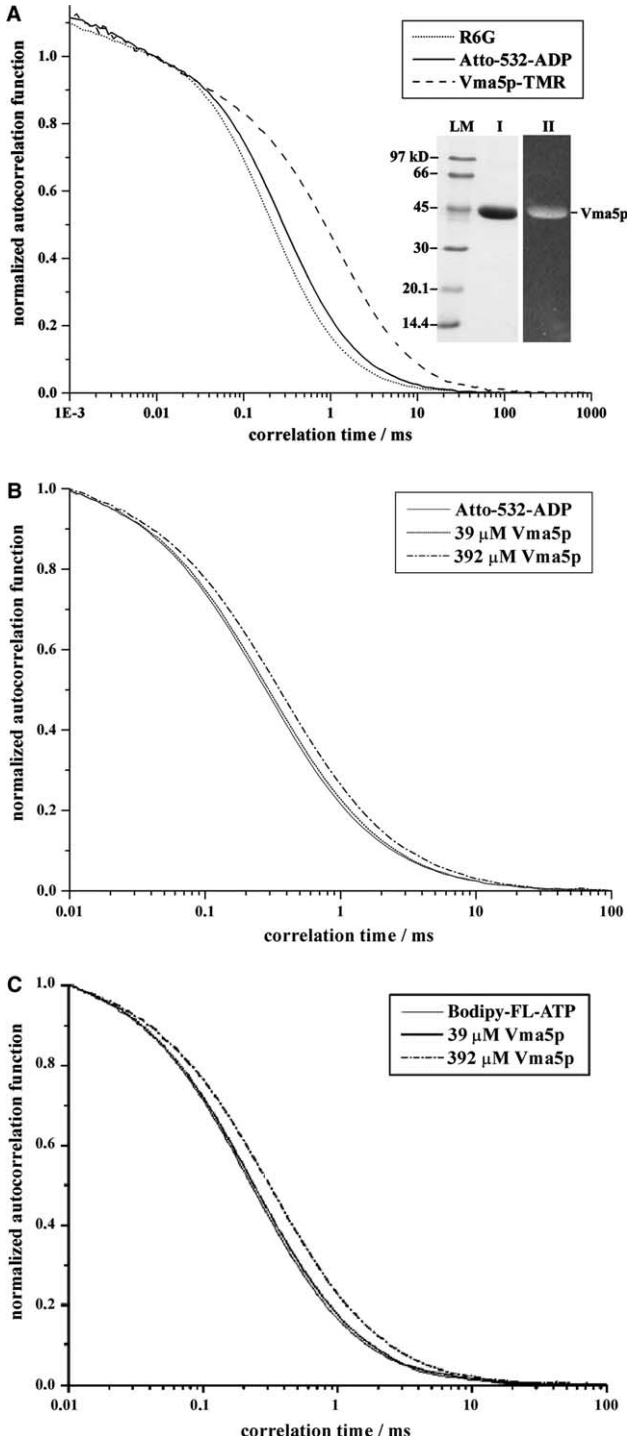

Fig. 4. Fluorescence correlation spectroscopy of VMA5p-TMR and the fluorescent ATP-analogues Atto-532-ADP and BODIPY-FL-ATP in the presence of 3.8 mM Ca^{2+}. (A) Normalized autocorrelation functions of freely diffusing fluorophore R6G (dotted curve), labeled Vma5p-TMR (dashed curve), and Atto-532-ADP (solid line). SDS–PAGE analysis of the TMR-labeled protein on the single Cys_{340} residue is displayed in the inset. Vma5p was incubated for 30 min with tetramethylrhodamine-maleimide (TMR). (B) Normalized autocorrelation functions of Atto-532-ADP (—), Atto-532-ADP in the absence and presence of 39 μM subunit C (···) and 392 μM (– – –), respectively. (C) Normalized autocorrelation functions of Bodipy-FL-ATP. (—) Bodipy-FL-ATP in the absence and presence of 39 μM subunit C (···) and 392 μM (– – –), respectively.

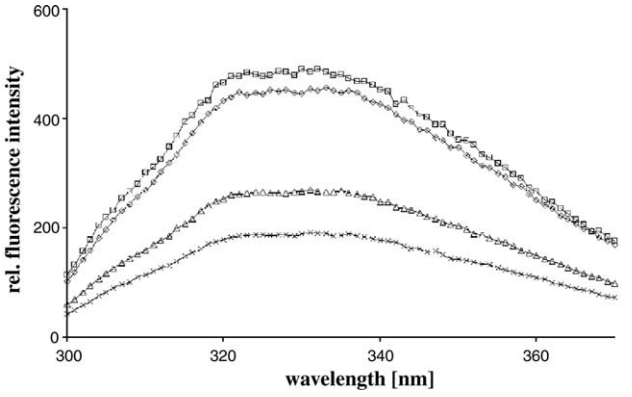

Fig. 5. Fluorescence emission spectra of Vma5p in the absence and presence of nucleotides. The tryptophan fluorescence emission spectrum of subunit C was measured with a 1:1 ratio of Ca^{2+} to nucleotide at room temperature. The protein was diluted in 50 mM, pH 8.5, and 100 mM NaCl and incubated with 2 mM (final concentration) of CaAMP · PNP (curve ×), CaATP (curve △) and CaADP (curve ◇) on ice for 5 min. Curve □, subunit C in the absence of nucleotides. The spectra were recorded with the emission and excitation slits at 5 nm.

in water [22]. By comparison, when the fluorescent ATP-analogue, BODIPY-FL-ATP, was used the mean diffusion time also increased up to 30% (Fig. 4C). The increase of the diffusion time was due to the increase in the mass of the diffusing particle, when BODIPY-FL-ATP bound to Vma5p. The diffusion coefficient, D, of BODIPY-FL-ATP was calculated to be $(2.2 \pm 0.1) \times 10^{-6}$ cm^2/s. A binding constant of about 0.75 and 0.87 mM of bound ADP and ATP, respectively, was calculated. FCS measurements of Atto-532-ADP in the presence of the C subunit of *A. thaliana* indicated a similar binding behaviour of the nucleotide (data not shown).

3.4. Secondary structural alterations due to nucleotide-binding

To obtain additional information on possible secondary structure alterations in subunit C after nucleotide-binding the fluorescence emission of Vma5p with and without ligands was monitored using the intrinsic tryptophan fluorescence (Fig. 5). Addition of CaATP (curve △) decreased the quantum yield markedly (up to 45%). The fluorescence intensity drops further in the presence of the non-hydrolyzable ATP-analog CaAMP · PNP (curve ×). In contrast, Vma5p in the presence of CaADP (curve ◇) displayed a spectrum similar to that obtained in the absence of nucleotides with a slightly lower intensity. The data indicate that the tryptophan fluorescence spectrum of subunit C (Vma5p) is sensitive to nucleotide binding.

3.5. Nucleotide-dependent trypsin treatment of subunit C

Firm evidence that nucleotide-binding of subunit C affected its structure was also obtained from tryptic digest of the protein in the presence of CaATP, CaADP or in the absence of nucleotides. The time course of proteolysis was probed by SDS–PAGE (Fig. 6). Proteolysis of subunit C at the trypsin amount used (320:1, (w/w)), was characterized by a rapid cleavage yielding the three major fragments (I–III), with apparent molecular masses of 26, 22 and 13 kDa, respectively. By contrast, nucleotide-binding of subunit C caused a slower cleavage of the protein and it became remarkably stable toward the proteolytic activity of trypsin.

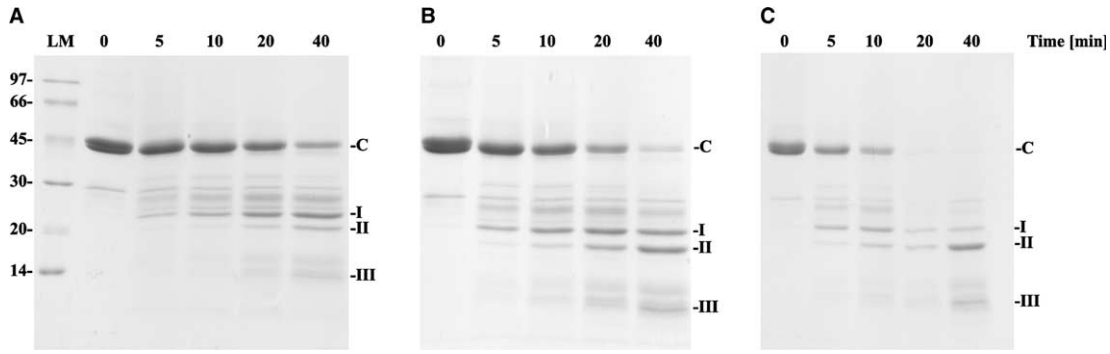

Fig. 6. Electrophoretic analysis of nucleotide dependent trypsin cleavage of Vma5p. (A) Subunit C was incubated for 5 min on ice with 2 mM CaATP (A), CaADP (B) or without nucleotides (C) before trypsin cleavage (ratio of subunit C:trypsin was 320:1 (w/w)) for the indicated time. Proteolysis was stopped by addition of the protease inhibitor Pefabloc SC to a final concentration of 4 mM. Samples were electrophoresed on a 17.5% total acrylamide and 0.4% cross-linked acrylamide gel and stained with Coomassie Blue G250.

There was, however, a difference in cleavage of this subunit depending on whether CaATP or CaADP is bound. Quantitation of the scanned C-bands indicated that 12% and 2% of this subunit remained after 40 min when CaATP or CaADP, respectively, bound to the protein. Furthermore, the ratio of the cleavage fragments I–III are 4:1:0.2, 1:1.5:0.3 and 1:4:0.5 in the presence of CaATP, CaADP and in the absence of nucleotides, respectively, indicating the altered accessibility of subunit C to trypsin in the absence and presence of different nucleotides.

4. Discussion

Metabolic control of ion-transport provides a means to reduce cellular ATP consumption during limited metabolic substrate or oxygen availability but also plays an important role in regulating transport during substrate availability. Recent studies have demonstrated that the metabolic substrate glucose activates V-ATPase activity through a pathway requiring aerobic glycolysis [24], whereby glucose deprivation induces disassembly of the V_1 and V_0 section [5]. Subunit C (Vma5p) is the only V-ATPase subunit that reversibly leaves the enzyme after removal of glucose, causing the catalytic subcomplex, V_1, to detach from the V_0 section. It has been hypothesized that subunit C plays a central role in the reversible reassembly of both domains [9,12] by binding as an anchor protein to the actin-based cytoskeleton and controlling the linkage of the cytoplasmic V_1 complex with the F- and/or G-actin [12,25]. The high-resolution structure of Vma5p (Fig. 1, [14]), composed of an upper head domain, a large globular foot, and an elongated neck domain, which connects the head and foot region, provide interfaces to interact with other V_1, V_0 subunits and actin. Both the head and foot domain show similar structural motives like the actin-binding protein gelsolin [14]. In this context it is of interest that besides potential actin binding both C subunits, Vma5p (*S. cerevisiae*) and VHA-C (*A. thaliana*), are able to bind the nucleotides ADP and ATP, as demonstrated by the photosensitive ADP-, ATP analogues and the fluorescent ADP-, ATP analogues described above, indicating the generality of nucleotide-binding to subunit C of V-ATPases. CNBr-cleavage of the photolabeled Vma5p and subsequent N-terminal sequencing of the marked peptides yielded that the nucleotide-binding site was located in the C-terminus, formed by the structural motive β–α–β–α, spanning amino acids 320–357 and 382–392. (Note, the amino acids 358–381 were not solved in the crystallographic structure [14].) This assignment is supported by the labeling experiments of *A. thaliana* subunit C mutants S221G, S223G and R318A:Y319A, P322A (numbering of analogous *S. cerevisiae*), showing that nucleotide binding was prevented by amino acid substitutions in the C-terminal region of subunit C (VHA-C). Site-directed mutagenesis revealed that the C-terminal region of Vma5p might be important for stable assembly of V_1 and V_0 [26]. In addition, binding of different maleimides to the single Cys_{340}, located at the point of the foot region of Vma5p, prevents this subunit from interaction with C-depleted V_1 [27], implying that this C-terminal domain forms at least partially the surface for binding to the stalk region of V_1. This surface in the foot of Vma5p is close to one of the proposed actin-binding sites of the protein. Therefore, binding of the nucleotides ADP and ATP to the C-terminus may induce structural changes in the foot region and thereby alters the interaction with other V_1,V_0 subunits and actin. The fluorescence quenching after addition of CaADP, -ATP or -AMP · PNP suggests secondary structural changes in subunit C in response to nucleotide binding. The fact that binding of CaADP resulted in a significant lower fluorescent quenching compared to CaATP and the non-hydrolyzable ATP, indicates that ADP and ATP induced different alterations in the Vma5p molecule. Furthermore, evidence for structural changes in subunit C, depending whether CaATP, -ADP or no nucleotide is bound to the protein, is provided by the different cleavage pattern of Vma5p after trypsin treatment (Fig. 6A–C).

The fact that subunit C is a nucleotide- and may be an actin-binding protein raises the possibility that this subunit senses the varying cellular ATP-concentration and might thereby induce the regulation of the reversible V_1V_0 disassembly. As described recently, the cytosolic ATP/ADP ratio is proposed to be an important parameter for controlling V-ATPase activity [28]. Using patch clamping of the *S. cerevisiae* vacuoles, it has been shown, that cytosolic ADP (5 mM) interacts with the V-ATPase and inhibits H^+-transport. In this study, addition of ADP on top of present MgATP resulted in a fast reduction of current. The effect of ADP was also investigated on the tonoplast V-ATPase, showing that this nucleotide acted as an inhibitor of ATP hydrolysis [29]. In this study the significance of the inhibition by ADP for the V-ATPase activity in vivo was tested by simulating the changes in cytosolic ATP and ADP ratio which occurs when darkened leaves are transferred into

light. The data yielded, that ATP hydrolysis rates increased when the ATP to ADP ratio increased from 2.9 in the dark to 9.4 after illumination [29]. Since subunit C plays a role in assembly [12] and stabilization [30] of V_1V_0 and in the regulation of V-ATPase activity in V_1 and V_1V_0 [13,15,16], the question arises whether the reduction of H^+-transport due to ADP, may be caused by ADP-binding to subunit C, resulting in altered interactions with V_1 and V_0 subunits and thereby reducing H^+-pump activity. In this context it should be mentioned that the fluorescent ATP-analogue bound slightly weaker to Vma5p than to the ADP-analogue, which is in line with the strong signal of the bound photoaffinity analogue 8-N_3-3′-biotinyl-ADP (Fig. 2B), compared with the 8-N_3-3′-biotinyl-ATP labeled Vma5p (Fig. 2A). Taken together, these results imply, that not only different structural changes due to binding of different nucleotides, but also the binding properties of these nucleotides might regulate the stalk subunit C, and with that the V_1V_0 ATPase. It has been proposed that the head domain of Vma5p is bound to the catalytic domain of V_1 and the foot region of Vma5p is oriented to the membrane portion [13,14,27]. The elongated feature of subunit C supports its role as a mediator, which facilitates the linkage of V_1 and V_0 and thereby permits alterations in the V_1V_0 ATPase due to nucleotide-binding. The data presented imply that subunit C in V_1V_0 acts not only as a stabilizer and regulator, but also as a sensor of the cytosolic ATP/ADP ratio.

Acknowledgements: We are grateful to G. Bernardy and I. Schäfer (Universität des Saarlandes) for skillful technical assistance and to M. Düser (Universität Stuttgart) for her support in FCS-measurements. We thank Dr. W. Nastainczyk (Universität des Saarlandes) for amino acid sequencing and Prof. H.-J. Schäfer (Universität Mainz) for the generous gift of 8-N_3-3′-biotinyl-ATP and 8-N_3-3′-biotinyl-ADP. This research was supported by a grant from the Deutsche Forschungsgemeinschaft to G.G. (GR 1475/9-1 and GR 1475/9-2) and K.S. (SFB446).

References

[1] Bowman, B.J. and Bowman, E.J. (1997) Mitochondrial and vacuolat ATPases in: The Mycota, III. Biochemistry and Molecular Biology (Brambl, R. and Marzluf, G., Eds.), pp. 57–83, Springer, Berlin.
[2] Nishi, T. and Forgac, M. (2002) The vacuolar (H+)-ATPases – nature's most versatile proton pumps. Nat. Rev. Mol. Cell. Biol. 3, 94–103.
[3] Nelson, N. (2003) A journey from mammals to yeast with vacuolar H^+-ATPase (V-ATPase). J. Bioenerg. Biomembr. 35, 281–290.
[4] Sumner, J.P., Dow, J.A.T., Earley, F.G., Klein, U., Jäger, D. and Wieczorek, H. (1995) Regulation of plasma-membrane V-ATPase activity by dissociation of peripheral subunits. J. Biol. Chem. 270, 5649–5653.
[5] Kane, P.M. (1995) Disassembly and reassembly of the yeast vacuolar H^+-ATPase in-vivo. J. Biol. Chem. 270, 17025–17032.
[6] Curtis, K.K. and Kane, P.M. (2002) Novel vacuolar H^+-ATPase complexes resulting from overproduction of Vma5p and Vma13p. J. Biol. Chem. 277, 2716–2724.
[7] Sagermann, M., Stevens, T.H. and Matthews, B.W. (2001) Crystal structure of the regulatory subunit H of the V-type ATPase of *Saccharomyces cerevisiae*. Proc. Natl. Acad. Sci. USA 98, 7134–7139.
[8] Wilkens, S., Inoue, T. and Forgac, M. (2004) Three-dimensional structure of the vacuolar ATPase. J. Biol. Chem. 279, 41942–41949.
[9] Kane, P.M. and Smardon, A.M. (2003) Assembly and regulation of the yeast vacuolar H^+-ATPase. J. Bioenerg. Biomembr. 35, 313–322.
[10] Grüber, G. (2000) Structural and functional features of the *Escherichia coli* F_1 ATPase. J. Bioenerg. Biomembr. 32, 341–346.
[11] Radermacher, M., Ruiz, T., Wieczorek, H. and Grüber, G. (2001) The structure of the V(1)-ATPase determined by three-dimensional electron microscopy of single particles. J. Struct. Biol. 135, 26–37.
[12] Vitavska, O., Wieczorek, H. and Merzendorfer, H. (2003) A novel role for subunit C in mediating binding of the H^+-V-ATPase to the actin cytoskeleton. J. Biol. Chem. 278, 18499–18505.
[13] Armbrüster, A., Svergun, D.I., Coskun, Ü., Juliano, S., Bailer, S.M. and Grüber, G. (2004) Structural analysis of the stalk subunit Vma5p of the yeast V-ATPase in solution. FEBS Lett. 570, 119–125.
[14] Drory, O., Frolow, F. and Nelson, N. (2004) Crystal structure of yeast V-ATPase subunit C reveals its stator function. EMBO Rep. 5, 1148–1152.
[15] Peng, S.B., Zhang, Y., Tsai, S.J., Xie, X.S. and Stone, D.K. (1994) Reconstitution of recombinant 33-kDa subunit of the clathrin-coated vesicle H^+-ATPase. J. Biol. Chem. 269, 11356–11360.
[16] Sun-Wada, G.-H., Murata, Y., Namba, M., Yamamoto, A., Wada, Y. and Futai, M. (2003) Mouse proton pump ATPase C subunit isoforms (C2-a and C2-b) specifically expressed in kidney and lung. J. Biol. Chem. 278, 44843–44851.
[17] Schäfer, H.-J., Coskun, Ü., Eger, O., Godovac-Zimmermann, J., Wieczorek, H., Kagawa, Y. and Grüber, G. (2001) 8-N_3-3′-biotinyl-ATP, a novel mono-functional reagent: Differences of the F_1 and V_1-ATPases by means of the ATP analogue. Biochem. Biophys. Res. Commun. 286, 1218–1227.
[18] Towbin, H., Staehelin, T. and Gordon, J. (1979) Electrophoretic transfer of proteins from polyacrylamide gels to nitrocellulose sheets: procedure and some applications. Proc. Natl. Acad. Sci. USA 76, 4350–4354.
[19] Matsudaira, P. (1987) Sequence from picomole quantities of proteins electroblotted onto polyvinylidene difluoride membranes. J. Biol. Chem. 262, 10035–10038.
[20] Börsch, M., Turina, P., Eggeling, C., Fries, J.R., Seidel, C.A.M., Labahn, A. and Gräber, P. (1998) Conformational changes of the H^+-ATPase from *Escherichia coli* upon nucleotide binding detected by single molecule fluorescence. FEBS Lett. 437, 251–254.
[21] Boldt, F.-M., Heinze, J., Petersen, J., Diez, M. and Börsch, M. (2004) Real-time pH microscopy down to the molecular level by combined scanning electrochemical microscopy/single-molecule fluorescence spectroscopy. Anal. Chem. 76, 3473–3481.
[22] Widengren, J., Mets, U. and Rigler, R. (1995) Fluorescence correlation spectroscopy as a tool to investigate chemical reactions in solutions and on cell surfaces. J. Phys. Chem. 99, 13368–13379.
[23] Knoche, M., Monnich, K., Schäfer, H.-J. and Kopperschläger, G. (2001) Photoaffinity labeling and photoaffinity cross-linking of phosphofructokinase-1 from Saccharomyces cerevisiae by 8-azidoadeninenucleotides. Arch. Biochem. Biophys. 385, 301–310.
[24] Nakamura, S. (2004) Glucose activates H(+)-ATPase in kidney epithelial cells. AJP-Cell Physiol. 287, C97–C105.
[25] Vitavska, O., Merzendorfer, H. and Wieczorek, H. (2004) The V-ATPase subunit C binds to polymeric F-actin as well as to monomeric G-actin and induces cross-linking of actin filaments. J. Biol. Chem. 280, 1070–1076.
[26] Curtis, K.K., Francis, S.A., Oluwatosin, Y. and Kane, P.M. (2002) Mutational analysis of the Subunit C (Vma5p) of the Yeast Vacuolar H^+-ATPase. J. Biol. Chem. 277, 8979–8988.
[27] Chaban, Y., Juliano, S., Boekema, E.J., and Grüber, G. (2004). Interaction between subunit C (Vma5p) of the yeast vacuolar ATPase and the stalk of the C-depleted V_1 ATPase from *Manduca sexta* Midgut. Biochim. Biophys. Acta (in press).
[28] Kettner, C., Obermeyer, G. and Bertl, A. (2003) Inhibition of the yeast V-type ATPase by cytosolic ADP. FEBS Lett. 535, 119–124.
[29] Dietz, K.-J., Heber, U. and Mimura, T. (1998) Modulation of the vacuolar H^+-ATPase by adenylates as basis for the transient CO_2-dependent acidification of the leaf vacuole upon illumination. Biochim. Biophys. Acta 1373, 87–92.
[30] Schumacher, K., Vafedos, D., McCarthy, M., Sze, H., Wilkins, T. and Chory, J. (1999) The *Arabidopsis* det3 mutant reveals a central role for the vacuolar H(+)-ATPase in plant growth and development. Genes Dev. 13, 3259–3270.
[31] Laemmli, U.K. (1970) Cleavage of structural proteins during the assembly of the head of bacteriophage T4. Nature 227, 680–685.